[12] C. M. Clark, J. A. Schneider, B. J. Bedell, T. G. Beach, W. B. Bilker, M. A. Mintun, M. J. Pontecorvo, F. Hefti, A. P. Carpenter, M. L. Flitter, M. J. Krautkramer, H. F. Kung, R. E. Coleman, C. H. Sadowsky, E. M. Reiman, S. P. Zehntner, D. M. Skovronsky, *JAMA* **2011**, *305*, 275–284.
[13] K. Herholz, K. Ebmeier, *Lancet Neurol.* **2011**, *10*, 667–70.
[14] V. L. Villemagne, K. E. Pike, G. Chételat, K. A. Ellis, R. S. Mulligan, P. Bourgeat, U. Ackermann, G. Jones, C. Szoeke, O. Salvado, R. Martins, G. O'Keefe, C. A. Mathis, W. E. Klunk, D. Ames, C. L. Masters, C. C. Rowe, *Ann. Neurol.* **2011**, *69*, 181–92.
[15] V. M. Lee, B. J. Balin, L. Otvos, J. Q. Trojanowski, *Science* **1991**, *251*, 675–8.
[16] R. Medeiros, D. Baglietto-Vargas, F. M. LaFerla, *CNS Neurosci. Ther.* **2011**, *17*, 514–24.
[17] P. V. Arriagada, J. H. Growdon, E. T. Hedley-Whyte, B. T. Hyman, *Neurology* **1992**, *42*, 631–631.
[18] D. W. Dickson, *Neurobiol. Aging* **1997**, *18*, S21–S26.
[19] P. T. Nelson, G. A. Jicha, F. A. Schmitt, H. Liu, D. G. Davis, M. S. Mendiondo, E. L. Abner, W. R. Markesbery, *J. Neuropathol. Exp. Neurol.* **2007**, *66*, 1136–46.
[20] P. T. Nelson, I. Alafuzoff, E. H. Bigio, C. Bouras, H. Braak, N. J. Cairns, R. J. Castellani, B. J. Crain, P. Davies, K. Del Tredici, C. Duyckaerts, M. P. Frosch, V. Haroutunian, P. R. Hof, C. M. Hulette, B. T. Hyman, T. Iwatsubo, K. A. Jellinger, G. A. Jicha et al., *J. Neuropathol. Exp. Neurol.* **2012**, *71*, 362–81.
[21] L. E. Rojo, J. Alzate-Morales, I. N. Saavedra, P. Davies, R. B. Maccioni, *J. Alzheimers Dis.* **2010**, *19*, 573–89.
[22] V. Villemagne, S. Furumoto, M. T. Fodero-Tavoletti, R. Harada, R. S. Mulligan, Y. Kudo, C. L. Masters, K. Yanai, C. C. Rowe, N. Okamura, *Future Neurol.* **2012**, *7*, 409–421.
[23] D. T. Chien, S. Bahri, A. K. Szardenings, J. C. Walsh, F. Mu, M.-Y. Su, W. R. Shankle, A. Elizarov, H. C. Kolb, *J. Alzheimer's Dis.* **2013**, *34*, 457–68.
[24] C.-F. Xia, J. Arteaga, G. Chen, U. Gangadharmath, L. F. Gomez, D. Kasi, C. Lam, Q. Liang, C. Liu, V. P. Mocharla, F. Mu, A. Sinha, H. Su, A. K. Szardenings, J. C. Walsh, E. Wang, C. Yu, W. Zhang, T. Zhao et al., *Alzheimer's Dement.* **2013**, *in press*, doi: 10.1016/j.jalz.2012.11.008.
[25] W. Zhang, J. Arteaga, D. K. Cashion, G. Chen, U. Gangadharmath, L. F. Gomez, D. Kasi, C. Lam, Q. Liang, C. Liu, V. P. Mocharla, F. Mu, A. Sinha, A. K. Szardenings, E. Wang, J. C. Walsh, C. Xia, C. Yu, T. Zhao et al., *J. Alzheimer's Dis.* **2012**, *31*, 601–12.
[26] N. Okamura, T. Suemoto, S. Furumoto, M. Suzuki, H. Shimadzu, H. Akatsu, T. Yamamoto, H. Fujiwara, M. Nemoto, M. Maruyama, H. Arai, K. Yanai, T. Sawada, Y. Kudo, *J. Neurosci.* **2005**, *25*, 10857–62.
[27] M. T. Fodero-Tavoletti, N. Okamura, S. Furumoto, R. S. Mulligan, A. R. Connor, C. A. McLean, D. Cao, A. Rigopoulos, G. A. Cartwright, G. O'Keefe, S. Gong, P. A. Adlard, K. J. Barnham, C. C. Rowe, C. L. Masters, Y. Kudo, R. Cappai, K. Yanai, V. L. Villemagne, *Brain* **2011**, *134*, 1089–100.
[28] N. Okamura, S. Furumoto, R. Harada, T. Tago, T. Yoshikawa, M. Fodero-Tavoletti, R. S. Mulligan, V. L. Villemagne, H. Akatsu, T. Yamamoto, H. Arai, R. Iwata, K. Yanai, Y. Kudo, *J. Nucl. Med.* **2013**, *54*, 1420–7.
[29] OECD GUIDELINE FOR THE TESTING OF CHEMICALS, Partition coefficient (n-octanol/water), high performance liquid chromatography (HPLC) method, doi: 10.1787/9789264069824-en.
[30] S. Barghorn, E. Mandelkow, *Biochemistry* **2002**, *41*, 14885–96.
[31] N. Okamura, T. Suemoto, H. Shimadzu, M. Suzuki, T. Shiomitsu, H. Akatsu, T. Yamamoto, M. Staufenbiel, K. Yanai, H. Arai, H. Sasaki, Y. Kudo, T. Sawada, *J. Neurosci.* **2004**, *24*, 2535–41.
[32] M. Biancalana, S. Koide, *Biochim. Biophys. Acta 2010*, **1804**, 1405–12.
[33] A. Forsberg, A. Juréus, Z. Cselényi, M. Eriksdotter, Y. Freund-Levi, F. Jeppsson, B.-M. Swahn, J. Sandell, P. Julin, M. Schou, J. Andersson, P. Johnström, K. Varnäs, C. Halldin, L. Farde, S. Svensson, *Eur. J. Nucl. Med. Mol. Imaging* **2013**, *40*, 580–93.

Supporting information

Additional supporting information may be found in the online version of this article at the publisher's web site.

Eur J Nucl Med Mol Imaging (2014) 41:816–826
DOI 10.1007/s00259-013-2681-7

ORIGINAL ARTICLE

In vivo evaluation of a novel tau imaging tracer for Alzheimer's disease

Victor L. Villemagne · Shozo Furumoto · Michelle T. Fodero-Tavoletti · Rachel S. Mulligan · John Hodges · Ryuichi Harada · Paul Yates · Olivier Piguet · Svetlana Pejoska · Vincent Doré · Kazuhiko Yanai · Colin L. Masters · Yukitsuka Kudo · Christopher C. Rowe · Nobuyuki Okamura

Received: 14 October 2013 / Accepted: 20 December 2013 / Published online: 11 February 2014

Abstract
Purpose Diagnosis of tauopathies such as Alzheimer's disease (AD) still relies on post-mortem examination of the human brain. A non-invasive method of determining brain tau burden in vivo would allow a better understanding of the pathophysiology of tauopathies. The purpose of the study was to evaluate ^{18}F-THK523 as a potential tau imaging tracer.

Methods Ten healthy elderly controls, three semantic dementia (SD) and ten AD patients underwent neuropsychological examination, MRI as well as ^{18}F-THK523 and ^{11}C-Pittsburgh compound B (PIB) positron emission tomography (PET) scans. Composite memory and non-memory scores, global and hippocampal brain volume, and partial volume-corrected tissue ratios for ^{18}F-THK523 and ^{11}C-PIB were estimated for all participants. Correlational analyses were performed between global and regional ^{18}F-THK523, ^{11}C-PIB, cognition and brain volumetrics.
Results ^{18}F-THK523 presented with fast reversible kinetics. Significantly higher ^{18}F-THK523 retention was observed in the temporal, parietal, orbitofrontal and hippocampi of AD patients when compared to healthy controls and SD patients. White matter retention was significantly higher than grey matter retention in all participants. The pattern of cortical ^{18}F-THK523 retention did not correlate with Aβ distribution as assessed by ^{11}C-PIB and followed the known distribution of tau in the AD brain, being higher in temporal and parietal areas than in the frontal region. Unlike ^{11}C-PIB, hippocampal ^{18}F-THK523 retention was correlated with several cognitive parameters and with hippocampal atrophy.
Conclusion ^{18}F-THK523 does not bind to Aβ in vivo, while following the known distribution of paired helical filaments (PHF)-tau in the brain. Significantly higher cortical ^{18}F-THK523 retention in AD patients as well as the association of hippocampal ^{18}F-THK523 retention with cognitive parameters and hippocampal volume suggests ^{18}F-THK523 selectively binds to tau in AD patients. Unfortunately, the very high ^{18}F-THK523 retention in white matter precludes simple visual inspection of the images, preventing its use in research or clinical settings.

Keywords Alzheimer's disease · Tau imaging · Aβ Imaging · Neurodegeneration · Brain

Electronic supplementary material The online version of this article (doi:10.1007/s00259-013-2681-7) contains supplementary material, which is available to authorized users.

V. L. Villemagne · M. T. Fodero-Tavoletti · R. S. Mulligan · P. Yates · S. Pejoska · V. Doré · C. C. Rowe
Centre for PET, Austin Health, Melbourne, Australia

V. L. Villemagne · M. T. Fodero-Tavoletti · C. L. Masters
The Mental Health Research Institute, Melbourne, Australia

S. Furumoto · R. Harada · K. Yanai · N. Okamura
Department of Pharmacology, Tohoku University School of Medicine, Sendai, Japan

J. Hodges · O. Piguet
Neuroscience Research Australia, Sydney, Australia

J. Hodges · O. Piguet
The University of New South Wales, Sydney, Australia

V. Doré
Preventative Health Flagship, CSIRO ICT, Brisbane, Australia

Y. Kudo
Innovation of New Biomedical Engineering Center, Tohoku University, Sendai, Japan

V. L. Villemagne (✉)
Department of Nuclear Medicine and Centre for PET, Austin Health, 145 Studley Rd, Heidelberg, VIC 3084, Australia
e-mail: villemagne@petnm.unimelb.edu.au

Introduction

Most neurodegenerative conditions are characterized by the aggregation of a misfolded protein such as Aβ and tau in Alzheimer's disease (AD), transactive response (TAR) DNA binding protein 43 kDa (TDP-43) in some forms of frontotemporal lobar degeneration (FTLD) such as semantic dementia (SD) or α-synuclein in Parkinson's disease. Tauopathies are neurodegenerative diseases characterized by the pathological accumulation of aggregated tau. AD is the most common tauopathy and the leading cause of dementia [1], but tau deposits are also found in other variants of FTLD, such as progressive non-fluent aphasia (PNFA) or in some cases of behavioural frontotemporal dementia (bFTD) [2]. Other tauopathies include Down's syndrome, Guam parkinsonism-dementia complex, frontotemporal dementia with parkinsonism linked to chromosome 17, corticobasal degeneration, progressive supranuclear palsy and chronic traumatic encephalopathy [3–5]. Definitive diagnosis of these neurodegenerative conditions can only be established after death. While these tauopathies share tau immunoreactivity in post-mortem brain examination, these tau aggregates can be composed of different tau isoforms displaying very distinct histopathological and ultrastructural differences [3, 6, 7]. In AD, these tau deposits can be recognized histologically as neurofibrillary tangles (NFTs) and neuropil threads as well as dystrophic neurites in senile plaques, whilst ultrastructurally they aggregate in paired helical filaments (PHF) [3, 4, 8]. While the underlying mechanisms leading to tau hyperphosphorylation, misfolding and aggregation remain unclear, tau aggregation and deposition follows a stereotypical and spatiotemporal pathway both at the intraneuronal level [8, 9] as well as in its topographical and neuroanatomical distribution in the brain [4, 10, 11].

The notion that tau dysregulation is a key mediator of neurodegeneration [12, 13] has stimulated the development of therapeutics for the treatment of AD and non-AD tauopathies [14–16]. Given these treatments are currently being developed, a non-invasive method of determining the tau burden in the brain would allow a better understanding of the pathophysiology of AD, FTLD and other tau-related neurodegenerative conditions. It will also lead to improvements in differential diagnostic accuracy and accelerate drug discovery by facilitating patient selection and monitor efficacy in novel anti-tau therapeutic trials. It would assist in the early and differential diagnosis of AD and non-AD tauopathies, while helping ascertain the relationship between the spatiotemporal distribution of tau aggregates in the brain to cognition and brain volumetrics. Development of tau imaging probes poses several more challenges than those associated with Aβ imaging, and these are mainly related to the idiosyncrasies of tau aggregation and deposition. In contrast to Aβ, most tau aggregates are intracellular, there are six tau isoforms and the different combinations of these isoforms manifest as different clinical phenotypes. Tau aggregates undergo a wide spectrum of post-translation modifications that, in addition to the combination of different isoforms, lead to diverse ultrastructural conformations and typical pathological lesions. Furthermore, tau aggregates coexist with other misfolded proteins sharing the same β-sheet secondary structure, as is in the case of AD where tau and Aβ are both co-localized in grey matter areas, where the concentrations of Aβ are, depending on the brain region, ~5–20 times higher than those of tau (for an in depth review see Villemagne et al. [17]).

In recent years, the main focus has been the development of selective ligands that allow early detection of Aβ deposition [18]. Among these tracers, ^{18}F-FDDNP was reported to non-selectively bind to both Aβ deposits and NFTs [19]. Phenylquinoline derivatives binding with high affinity and selectivity for tau aggregates have been developed as candidates for tau imaging agents at Tohoku University in Sendai, Japan [20]. Among them, ^{18}F-THK523 (THK523) was the first reported selective tau imaging tracer that can non-invasively detect tau deposits in a transgenic mouse brain [21]. This report was recently followed by several other potential tau tracer candidates [22–27].

After a careful in vitro evaluation, the initial in vivo characterization of a novel positron emission tomography (PET) neuroligand candidate requires to fulfill certain conditions such as safety at low tracer doses, possess high affinity and selectivity for the target, ability to cross the blood–brain barrier, display low non-specific binding with adequate regional distribution and its relation to parameters known to be associated with the intended target, suitable brain kinetics, lack of problematic radiolabelled metabolites [28] before it is applied to research or clinical use (Supplementary Fig. 1).

Therefore, the main objective of the present study was to characterize the in vivo suitability of THK523 for tau imaging in humans. The in vivo assessment comprised: (a) comparing the global and regional THK523 binding in healthy controls (HC), AD and SD patients, (b) assessing the relationship between THK523 retention and cognition, (c) assessing the relationship between THK523 retention and brain volumetrics and (d) comparing the regional brain distribution of THK523 with that of ^{11}C-Pittsburgh compound B (PIB) in the same participants.

Materials and methods

Participants

Written informed consent was obtained from all participants. Approval for the study was obtained from the Austin Health Human Research Ethics Committee. Elderly HC were recruited by advertisement in the community and dementia patients

were recruited from tertiary Memory Disorders Clinics or from physicians who sub-specialize in dementia care. All participants were classified on the basis of their clinical and neuropsychological performance by consensus of a neurologist and a neuropsychologist. Individuals classified as HC performed within normal limits on cognitive tests. AD patients met NINCDS-ADRDA criteria for probable AD [29], while three FTLD patients were classified as SD [30, 31]. None of the AD or FTLD patients had a family history of dementia.

Safety evaluation

Clinical, haematological and biochemical data on the safety of THK523 were collected for all participants. Heart rate, blood pressure, temperature and respiratory rate were measured immediately prior to injection and at 2, 15, 60 and 180 min post-injection. Immediately prior to THK523 injection, blood was drawn for routine haematology and biochemistry tests. An ECG was performed prior to injection of THK523 and at the completion of the scan, when they were also questioned for adverse events. All subjects were contacted by telephone 24 h later and questioned for adverse events. Between 5 and 8 days post-injection, subjects returned to be questioned for adverse events and for a physical examination, including a set of observations and repeat haematology and biochemistry testing.

Neuropsychological evaluation

In addition to the Mini-Mental State Examination (MMSE), Clinical Dementia Rating (CDR) and Clinical Dementia Rating Sum of Boxes (CDR SOB), the primary cognitive performance measures were composite episodic memory and non-memory scores generated as previously described [32]. Briefly, a composite episodic memory score was calculated by taking the average of the z scores (generated using 65 HC with both low PIB and normal MRI as the reference) for Rey Complex Figure Test (RCFT, 30 min) Long Delay and California Verbal Learning Test - Second Edition (CVLT-II) Long Delay and Logical Memory II. A composite non-memory score was calculated by taking the average of the z scores for the Boston Naming Test, letter fluency, category fluency, digit span forwards and backwards, digit symbol-coding and RCFT copy.

Image acquisition

Magnetic resonance imaging

Participants received an MRI on a 3 T Siemens TRIO MRI system (Siemens Healthcare, Erlangen, Germany) using the Alzheimer's Disease Neuroimaging Initiative (ADNI) 3D magnetization prepared rapid acquisition gradient echo (MPRAGE) sequence with 1×1 mm in-plane resolution and 1.2-mm slice thickness, repetition time (TR)/echo time (TE)/T1-weighted=2,300/2.98/900, flip angle 9° and field of view 240×256 and 160 slices. T2 -weighted fast spin-echo (FSE) and fluid-attenuated inversion recovery (FLAIR) sequences were also obtained. The interval between the THK523 and MRI studies was 1.6±3.3 months.

Positron emission tomography

Productions of ^{11}C-PIB and ^{18}F-THK523 were performed in the Centre for PET, Austin Hospital. ^{11}C-PIB was synthesized using the one-step ^{11}C-methyl triflate approach as previously described [18]. The decay-corrected average radiochemical yield for ^{11}C-PIB was 30 % with a radiochemical purity of >98 % and a specific activity of 30±7. 5 GBq/μmol. ^{18}F-THK523 was synthesized by nucleophilic substitution of the tosylate precursor [BF-241, 2-3 mg in 700 μl dimethyl sulphoxide (DMSO)]. The decay-corrected average radiochemical yield of the production of ^{18}F-THK523 was 22.5± 5 %, with a radiochemical purity of>95 % and a specific activity of 225.6±134.8 GBq/μmol (6.2±3.3 Ci/μmol).

A 30-min acquisition (6×5-min frames) on an Allegro™ PET camera started 40 min after injection of 300 MBq ^{11}C-PIB intravenously. A 90-min list-mode emission acquisition was performed in 3D mode after injection of 200 MBq ^{18}F-THK523. List-mode raw data were sorted offline into 6×30-s, 7×1-min, 4×2.5-min, 2×5-min and 6×10-min frames. The sorted sinograms were reconstructed using a 3D row action maximum likelihood algorithm (RAMLA). The interval between the THK523 and PIB PET studies was 0.3±3.8 months.

Tracer metabolism

Compound stability was assessed by incubating the tracer for 5, 30, 60, 90, 180 and 240 min with human S9 liver fractions.

Image analysis

Magnetic resonance imaging

Hippocampal and cortical grey matter volumes were obtained using a commercial fully automated volumetric measurement program (NeuroQuant®) applied to the 3D MPRAGE MRI images. The primary MRI performance measures were the grey cortical matter and hippocampal volumes normalized for total intracranial volume.

Positron emission tomography

PET images were processed using a semi-automatic region of interest (ROI) method as previously described [32]. Briefly,

THK523 and PIB PET images were co-registered to each individual's MRI using SPM8 (Wellcome Trust Centre for Neuroimaging, London, UK), and the same ROI template was applied. Given the reversible nature of THK523 kinetics, distribution volume ratios (DVR) were determined through graphical analysis of the dynamic data. Standardized uptake value ratios (SUVR) for PIB and THK523 as well as THK523 DVR were generated using the cerebellar cortex as reference region [18, 33]. Global tau and Aβ burden were expressed as the average SUVR for the following cortical ROIs: frontal (consisting of dorsolateral prefrontal, ventrolateral prefrontal and orbitofrontal regions), superior parietal, lateral temporal, lateral occipital and anterior and posterior cingulate for THK523 and PIB, respectively. As in previous studies, a PIB SUVR threshold of 1.5 was used to categorize high (PIB+) and low (PIB−) Aβ burden [32].

Partial volume correction (PVC), accounting for *both* grey matter atrophy and white matter spillover, was performed applying a three-compartment approach using PMOD 3.1 (PMOD Technologies Ltd., Zurich, Switzerland). DVR for THK523 were determined through graphical analysis of the last 45 min of the 90-min acquisition [33]. In order to avoid arterial blood sampling, a simplified approach was applied using the cerebellar cortex as reference region [18, 33]. Global DVR was calculated with the same regions used for the global SUVR. The primary outcome measure used for all THK523 and PIB assessments was the PVC SUVR.

Statistical evaluation

Normality of distribution was tested using the Shapiro-Wilk test and visual inspection of variable histograms. Statistical evaluations to establish differences between clinical groups means were performed using a Tukey-Kramer HSD test and by a Dunnett's test to compare each group with controls. Pearson's product-moment correlation analyses were conducted between imaging and clinical variables. Categorical differences were evaluated using Fisher's exact test. Effect size was measured with Cohen's *d*. All analyses were adjusted for age and corrected for multiple comparisons using false discovery rates. Data are presented as mean±standard deviation unless otherwise stated.

Results

Participants

Demographic characteristics of the participants are shown in Table 1. As expected, there were significant differences between the AD and SD patients and HC in cognitive performance and brain volumetrics. The AD group also presented with significantly higher PIB retention. While there were no significant differences between groups in age and gender, the AD group was less educated. While seven of the HC and the three SD patients showed low PIB retention, three of the HC presented with high PIB retention (Table 1).

No adverse events related to the study drug were observed or reported by participants or carers following the THK523 scan. There were no significant changes in clinical or biochemical parameters.

Tracer metabolism

THK523 was minimally metabolized, with 91, 81 and 65 % of unchanged parent compound remaining at 30, 90 and 180 min, respectively. No lipophilic radiometabolites were observed.

Brain kinetics

Brain THK523 radioactivity peaked between 3 and 6 min post-injection and the binding appeared to be reversible with rapid clearance from the brain (Fig. 1a, b). THK523 cleared fastest from cerebellar cortex and the clearance rate was the same for all groups (Fig. 1a, b). Clearance was slower from cortical areas in AD (Fig. 1b) than in HC (Fig. 1a) and SD patients. The ratio of cortical to cerebellar binding became constant in all participants by 50 min after injection (Fig. 1c).

Visual inspection

Visual inspection of the summed 60–90-min SUVR images revealed significantly higher THK523 retention in white matter than in grey matter regions, being significantly higher in AD patients than in HC or SD (Fig. 1d).

Assessment of tau burden

Regional analysis showed that there were no group differences in cerebellar cortex THK523 SUV, and there was no correlation between cerebellar cortex THK523 SUV with age in the whole cohort or with dementia severity in the AD group as assessed by MMSE (r=0.25, p=0.50), CDR (r=0.13, p=0.72) or CDR SOB (r=0.03, p=0.94).

While 60–90-min THK523 SUVR was estimated for all participants, four participants (two HC and two AD) were not able to complete the initial THK523 dynamic scan preventing calculation of DVR. In the remaining 16 subjects, significantly higher THK523 DVR were found in AD subjects in all cortical regions. The global THK523 DVR was 1.02±0.15 in AD vs 0.86±0.11 in HC (p=0.04, Cohen's effect size d=1.2). No significant differences were observed between HC and SD patients. Similar findings were observed with THK523

Table 1 Demographics

	HC (n=10)	SD (n=3)	AD (n=10)
Age	77.4±10.0	65.6±8.1	75.6±9.5
Gender (M/F)	3/7	1/2	4/6
MMSE	29.3±1.1	21.7±1.2*	16.7±6.6*
CDR	0.0	0.8±0.3*	1.3±0.6*
CDR SOB	0.1±0.2	2.5±1.1*	7.3±4.5*
Years of education	14.7±2.7	12.5±4.9	11.5±3.6*
Episodic memory scores	−0.4±0.6	−1.9±0.9*	−3.8±0.5*
Non-memory scores	−0.1±0.4	−1.4±1.2*	−3.4±1.6*
Hippocampal volume (cm^3)	5.1±0.6	4.3±0.3	4.1±1.0*
Aβ burden (PIB SUVR)	1.5±0.6	1.1±0.1	2.9±0.5*
	[PIB−=1.2±0.1 (n=7)]		
	[PIB+=2.2±0.6 (n=3)]		

MMSE Mini-Mental State Examination, *CDR* Clinical Dementia Rating, *CDR SOB* Clinical Dementia Rating Sum of Boxes, *PIB* Pittsburgh compound B, *SUVR* standardized uptake value ratio, *PIB−* low PIB retention, *PIB+* high PIB retention

*Significantly different from HC (p<0.05)

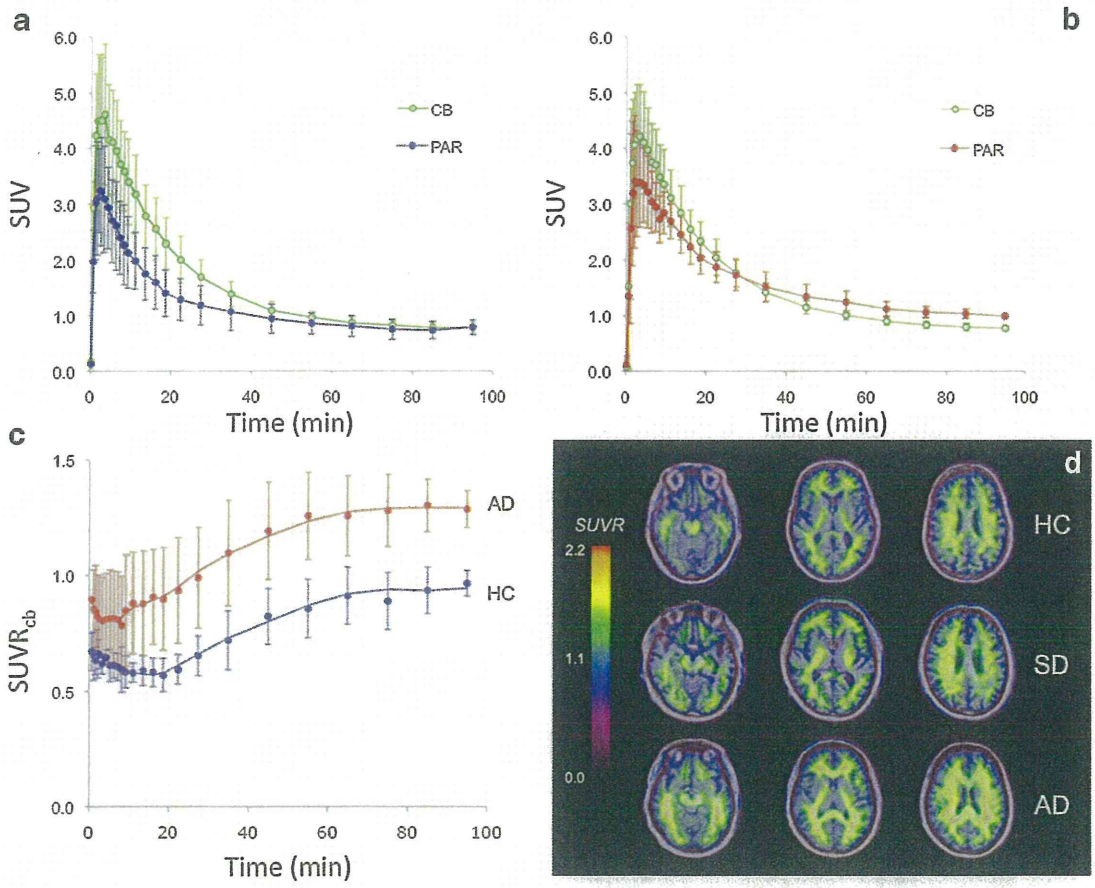

Fig. 1 ^{18}F-THK523 binding. Time-radioactivity curves for ^{18}F-THK523 in the parietal cortex (*PAR*) and the cerebellar grey matter (*CB*) in healthy controls (*HC*) (**a**) and Alzheimer's disease (*AD*) patients (**b**). There is fast ^{18}F-THK523 uptake in the brain followed by a fast clearance phase. While there is slower clearance with significantly higher retention in the parietal cortex of AD patients compared to HC, there are no significant differences in the cerebellar cortex uptake and clearance, further validating its use as reference region. **c** The total to non-specific binding ratios curves show significantly higher ^{18}F-THK523 retention in the parietal cortex of AD patients compared to HC. The specific binding reaches a plateau by 50 min post-injection. **d** Representative ^{18}F-THK523 PET images at three different brain levels in a 69-year-old female HC (MMSE 30, *top row*), a 73-year-old male semantic dementia (*SD*) patient (MMSE 21, *middle row*) and a 72-year-old female AD patient (MMSE 22, *bottom row*). Visual inspection of the images reveals no differences in ^{18}F-THK523 retention between HC and SD. There is higher white matter retention in AD compared to HC and SD. Data expressed as mean±SD of ten HC and ten AD patients

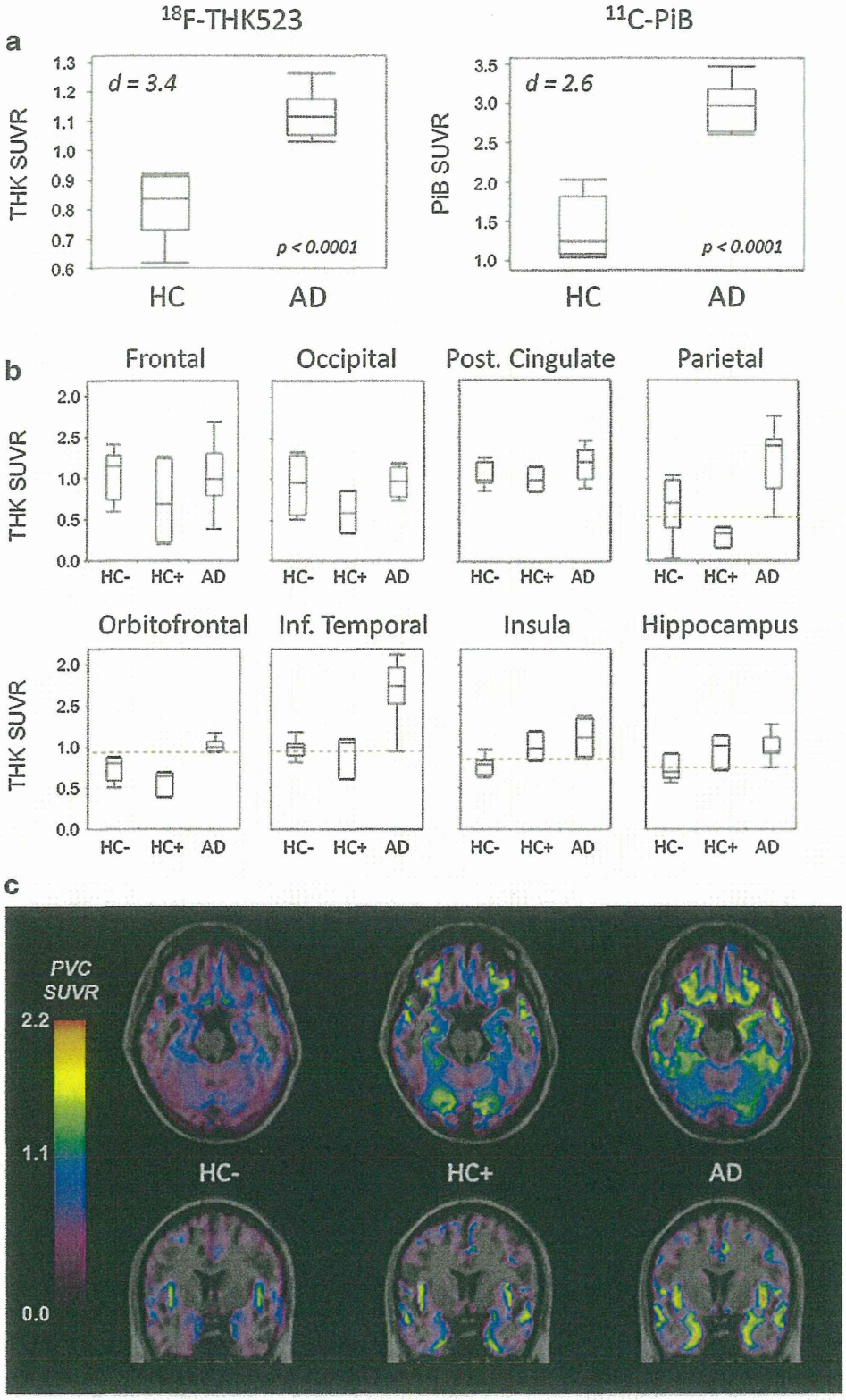

SUVR, and although SUVR values were higher than THK523 DVR, the rank order of the participants and the rank order of the regional values were identical, both showing the highest THK523 retention in temporal, parietal and hippocampus.

Table 2 Global and regional ^{18}F-THK523 and ^{11}C-PIB retention in AD

Region	THK SUVR				PIB SUVR			
	HC	AD	*p*	*d*	HC	AD	*p*	*d*
Frontal lobe	0.92±0.38	1.01±0.36	0.56	0.24	1.51±0.74	3.05±0.68	<0.0001	2.17
Orbitofrontal	0.68±0.16	1.06±0.24	<0.0001	1.87	1.42±0.50	2.91±0.58	<0.0001	2.74
Ant. cingulate	0.60±0.45	0.54±0.22	0.52	−0.19	1.61±0.75	2.98±0.59	<0.0001	2.04
Post. Cingulate	0.99±0.15	1.17±0.20	0.029	1.02	1.57±0.65	3.39±0.49	<0.0001	3.16
Parietal lobe	0.54±0.33	1.24±0.38	<0.0001	1.99	1.33±0.63	2.77±0.45	<0.0001	2.63
Lat. occipital lobe	0.81±0.33	0.91±0.29	0.38	0.31	1.35±0.35	2.32±0.38	<0.0001	2.66
Sup. temporal lobe	0.94±0.37	1.35±0.29	0.005	1.22	1.46±0.65	2.83±0.61	<0.0001	2.17
Inf. temporal lobe	0.96±0.16	1.81±0.58	<0.0001	2.00	1.52±0.62	2.89±0.51	<0.0001	2.42
Hippocampus	0.78±0.18	0.97±0.18	0.008	1.01	1.53±0.31	1.82±0.32	0.08	0.93
Insula	0.85±0.16	1.09±0.22	0.007	1.30	1.54±0.48	2.35±0.38	<0.0001	1.87
Striatum	0.39±0.16	0.46±0.25	0.65	0.33	1.79±0.76	2.98±0.64	0.0004	1.71
Subcortical white matter[a]	1.61±0.12	1.90±0.17	0.002	2.01	2.14±0.28	2.41±0.37	0.10	0.83
Neocortical	0.82±0.10	1.13±0.07	<0.0001	3.42	1.46±0.61	2.88±0.48	<0.0001	2.59

All images were partial volume corrected and then scaled and sampled. All results are adjusted for age
HC healthy control, *AD* Alzheimer's disease, *THK* ^{18}F-THK523, *PIB* ^{11}C-Pittsburgh compound B, *SUVR* standardized uptake value ratio, *d* Cohen's effect size *d*
[a] White matter SUVR are not partial volume corrected

THK523 SUVR correlated strongly with THK523 DVR in all cortical regions with a correlation coefficient of $r=0.85$ ($p<0.0001$) for the mean global measure.

Regional analysis of the non-partial volume-corrected images revealed significantly higher cortical THK523 retention in AD (Supplementary Fig. 2a) than in HC and SD patients. THK523 retention was also significantly higher in subcortical white matter in AD (Table 2). The spillover from the high retention in white matter was likely to contribute substantially to the radioactivity measured in grey matter; therefore, PVC of the images, correcting for *both* cortical grey matter atrophy and for white matter spillover, was performed. The PVC SUVR derived from the summed 60–90 min were subsequently used to assess THK523 retention as well as comparison with PIB and for correlation with brain volumetrics and cognitive parameters (Table 2). After PVC, while little or no THK523 retention was observed in cortical areas in HC, THK523 retention in AD patients was most prominent in cortical association areas, where only the temporal, parietal, hippocampal, orbitofrontal, and posterior cingulate regions (Supplementary Fig. 2b), brain areas known from post-mortem studies to contain substantial amounts of tau deposits in AD [10, 11], remained significant (Table 2). No significant differences were observed between HC and SD patients using either THK523 (Supplementary Table 1) or PIB (Supplementary Table 2). Global THK523 PVC SUVR in HC was 0.82±0.10 compared to 1.13±0.07 in AD ($p<0.0001$, Cohen's $d=3.4$) (Fig. 2).

◀ **Fig. 2** Global and regional retention of ^{18}F-THK523 and ^{11}C-PIB in AD. **a** Box plots for ^{18}F-THK523 (*left top panel*) and ^{11}C-PIB (*right top panel*) showing the global SUVR of both tracers. **b** When cognitively unimpaired HC with high (*HC+*) or low (*HC–*) ^{11}C-PIB retention were examined separately, it was observed that while ^{18}F-THK523 retention in isocortex of individuals with high ^{11}C-PIB retention aligned with those with low ^{11}C-PIB retention ^{18}F-THK523 retention in hippocampus and insula were not significantly different from the ^{18}F-THK523 retention in AD. *Red dotted lines* denote the bottom quartile of THK523 SUVR in AD patients. **c** Average parametric ^{18}F-THK523 transaxial and coronal partial volume-corrected (*PVC*) PET images overlaid on MRI of ten HC and ten AD patients, showing higher hippocampal and insular ^{18}F-THK523 retention on three HC with high (*HC+*) ^{11}C-PIB retention compared with seven HC with low (*HC–*) ^{11}C-PIB retention

Comparison of THK523 and PIB cortical retention

While seven of the ten HC and the three SD patients showed low Aβ burdens, all the AD patients and three HC presented with high Aβ burdens in the brain. In AD patients, the topographical pattern of cortical THK523 retention was clearly different from the cortical retention observed with PIB. While PIB was highest in the frontal, posterior cingulate, striatum and temporal cortices, THK523 was highest in temporal, parietal, hippocampus and posterior cingulate (Supplementary Fig. 3a). There was no correlation between the cortical THK523 SUVR and cortical PIB SUVR in the AD patients ($r=0.04$, $p=0.90$) (Supplementary Fig. 3b). Interestingly, in those HC with high Aβ burden (PIB+HC) while cortical THK523 retention was not significantly different to the cortical retention in PIB− HC, THK523 retention in the

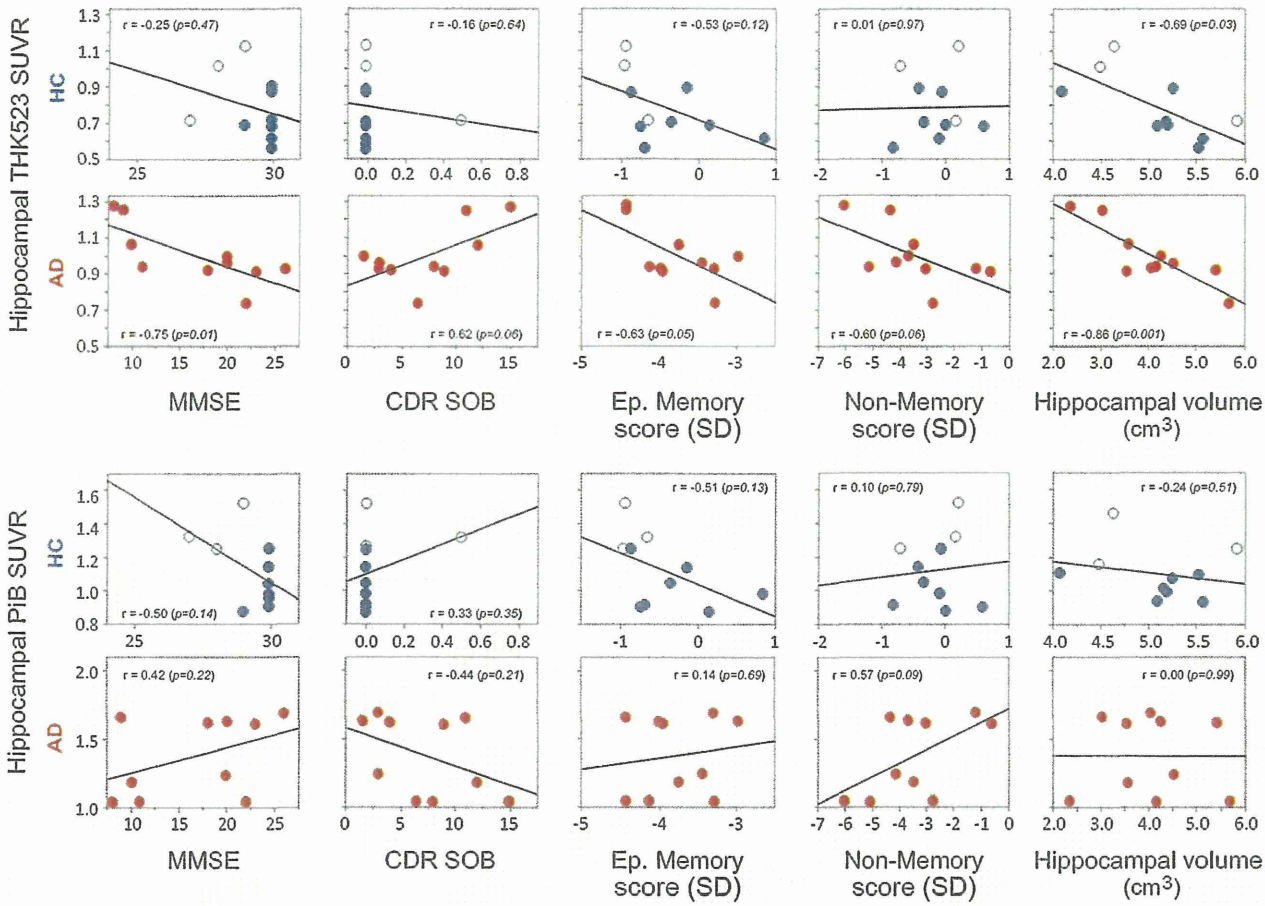

Fig. 3 Relationship between hippocampal ^{18}F-THK523 and ^{11}C-PIB retention with cognition and hippocampal volume. Regression analysis shows that while hippocampal ^{18}F-THK523 retention is not associated with cognition in HC, it is strongly associated with different cognitive parameters in AD patients (*top two rows*). On the other hand, hippocampal ^{18}F-THK523 retention is strongly associated with hippocampal volume in both HC and AD patients. There was no association between hippocampal ^{11}C-PIB retention (*bottom two rows*) with either cognitive parameters or hippocampal volume in any of the groups examined. All correlations were adjusted for age

hippocampus and insula was significantly higher than PIB–HC, but not significantly different from AD (Fig. 2).

Association between THK523 retention, cognition and brain volumetrics

While providing evidence of the general direction of the association between the different parameters (e.g. higher tau burden, lower cognitive performance), the associations derived from assessing all groups together tend to yield spurious correlations driven by the significant differences between the clinical groups. In order to avoid this issue, the associations with cognition and brain volumetrics were assessed in each clinical group separately.

In the case of THK523, there were no associations between cortical THK523 retention and cognitive parameters in HC, with the exception of the insula associated with episodic memory scores (r=−0.70, p=0.026). In the AD group, hippocampal THK523 retention was significantly associated with MMSE (r=−0.75, p=0.01) and episodic memory (r=−0.63, p=0.05) (Fig. 3). In the AD group, a strong trend was also observed between hippocampal THK523 retention, CDR SOB (r=0.62, p=0.055) and non-memory scores (r=−0.60, p=0.056). In regard to brain volumes, only hippocampal THK523 retention was significantly associated with hippocampal volume in both the HC (r=−0.69, p=0.03) and AD (r=−0.86, p=0.001) groups (Fig. 3). There were no correlations between global THK523 retention and cortical grey matter volume in any of the groups.

In the case of PIB, there were associations between PIB retention and MMSE in the orbitofrontal (r=−0.67, p=0.034), anterior (r=−0.65, p=0.04) and posterior cingulate (r=−0.78, p=0.007) regions of HC. In AD, there were some associations between PIB retention and cognitive parameters, but these correlations were, in every case, in the opposite direction as expected, where PIB retention in the anterior cingulate gyrus was positively associated with MMSE (r=0.63, p=0.049),

episodic memory (r=0.73, p=0.016) and non-memory scores (r=0.64, p=0.046) and inversely associated with CDR SOB (r=−0.68, p=0.03). There were no associations between hippocampal PIB retention and any cognitive parameter in any of the clinical groups (Fig. 3). There were no significant associations between global PIB retention and cortical grey matter volume in either HC or AD patients. In contrast to what was observed for hippocampal THK523 retention, there was no association between hippocampal PIB retention and hippocampal volume in any of the groups examined (Fig. 3).

Discussion

To the best of our knowledge, this is the first time a selective tau imaging agent has been thoroughly evaluated in human volunteers, assessing its associations with cognition and brain volumetrics, as well as a direct comparison with Aβ imaging using PIB.

Global cortical THK523 binding provided a very robust separation of AD patients from healthy elderly subjects (Cohen's d=3.4). Furthermore, cortical THK523 retention in AD patients followed the reported histopathological brain distribution of PHF-tau in AD [10, 11]. Examination of the brain kinetics of THK523 showed that it presents reversible binding kinetics, reaching apparent steady state about 50 min after injection of the radiotracer. Visual inspection of the THK523 images was hampered by the very high retention in white matter. In addition to the high non-specific binding, previous reports have demonstrated substantial concentrations of PHF-tau in white matter in AD [34, 35], suggesting THK523 retention in white matter might not solely reflect marked non-specific binding, but also some small degree of specific binding. Several factors were taken into account for the selection of the reference region. To date, no report has described tau deposition in the cerebellar cortex in sporadic AD [36]. There were no group differences in cerebellar cortex THK523 SUV, and there was no association between cerebellar cortex THK523 SUV with age in the whole cohort, or with dementia severity in the AD group, further supporting the use of the cerebellar cortex as reference region.

The regional brain distribution of THK523 showed a marked contrast when compared to that of PIB. While the highest PIB retention was observed in frontal, posterior cingulate, caudate and temporal cortices, the highest THK523 retention was observed in the inferior temporal, orbitofrontal, hippocampus, insula and parietal cortices. This was further confirmed by a lack of correlation between PIB SUVR and THK523 SUVR (r=0.04, p=0.90).

SD patients were included in the evaluation of THK523 as pathological controls [31]. Rather than tau aggregates, the vast majority of SD cases have been associated with the aggregation of TDP-43 [2, 31]. SD patients showed neither THK523 nor PIB retention in the brain (Supplementary Tables 1 and 2), suggesting the absence of both Aβ [37] and tau deposits in SD.

Three HC showed high cortical PIB retention (PIB+HC), consistent with previous PIB studies that have reported positive scans in 25–35 % of normal elderly individuals [38]. Despite the limited subsample size the finding is interesting because while cortical THK523 retention in PIB+HC was not significantly different from the cortical retention in PIB− HC, THK523 retention in the hippocampus and insula was significantly higher than in PIB− HC, but not significantly different from AD, suggesting that tau deposition in these regions might precede the dementia of AD [6, 39]. These findings might indicate that the combination of widespread cortical Aβ plus hippocampal tau deposition might not be enough to lead to significant cognitive impairment, requiring tau deposition in polymodal and unimodal association areas of the brain for objective cognitive impairment to be manifest [7, 10, 11].

As with Aβ imaging [40], longitudinal studies will assist in establishing the spatiotemporal patterns of tau deposition and help determine whether or not apparently healthy individuals with substantial hippocampal tau deposition will develop the AD phenotype, thus allowing very early, even preclinical diagnosis of AD, or if hippocampal tau deposits are just an age-associated process and only cortical tau deposition leads to cognitive impairment [39, 41].

In AD, hippocampal THK523 retention was associated with cognitive parameters. Similarly, hippocampal THK523 retention was associated with hippocampal volume in both HC and AD patients. Human post-mortem studies have shown that the density of NFTs strongly correlates with neurodegeneration and cognitive deficits, while Aβ plaque density does not [42, 43], a finding that was further confirmed through Aβ imaging studies [18, 32]. Furthermore, in stark contrast with Aβ plaques, NFTs are usually not present in associating cortical regions in cognitively unimpaired individuals [11, 18, 39].

As was previously reported in vitro [21, 44], several lines of evidence support the notion that THK523 selectively binds to PHF-tau and not to Aβ in vivo: (a) cortical THK523 retention is significantly higher in AD, following the known distribution of PHF-tau in the AD brain; (b) PIB and THK523 show different brain regional distribution patterns; (c) there is no correlation between PIB and THK523 retention; and (d) while hippocampal THK523 retention significantly correlates with cognitive parameters and hippocampal atrophy, hippocampal PIB retention does not.

While this was a first-in-human study, the limited sample size requires cautious interpretation of the findings. Furthermore, while our results suggest that ^{18}F-THK523 can reliably quantify PHF-tau deposition in vivo, there are serious limitations associated with the tracer itself. The high white matter THK523 retention, even if it might reflect some small degree of specific binding, precludes simple visual inspection of the